arXiv:hep-ph/0206013v4 11 Nov 2002

Exclusive B-meson Rare Decays and General Relations of Form Factors in Effective Field Theory of Heavy Quarks

M. Zhong†, Y.L. Wu† and W.Y. Wang*
† *Institute of Theoretical Physics, Academia Sinica, Beijing 100080, China*
∗ *Department of Physics, Tsinghua University, Beijing 100084, China*

Abstract

B meson rare decays ($B \to K(K^*)l\bar{l}$ and $B \to K^*\gamma$) are analyzed in the framework of effective field theory of heavy quarks. The semileptonic and penguin type form factors for these decays are calculated by using the light cone sum rules method at the leading order of $1/m_Q$ expansion. Four exact relations between the two types of form factors are obtained at the leading order of $1/m_Q$ expansion. Of particular, the relations are found to hold for whole momentum transfer region. We also investigate the validity of the relations resulted from the large energy effective theory based on the general relations obtained in the present approach. The branching ratios of the rare decays are presented and their potential importance for extracting the CKM matrix elements and probing new physics is emphasized.

PACS numbers: 11.20.Hv, 11.55.Hx, 12.39.Hg, 13.20.Fc, 13.20.He
Keywords: rare decay, CKM matrix elements, form factors, effective field theory, light cone sum rules

Typeset using REVTEX

I. INTRODUCTION

B meson rare decays $B \to K^*\gamma$ and $B \to K(K^*)\bar{l}l$ are induced by transitions $b \to s\gamma$ and $b \to s\bar{l}l$ via penguin loop diagrams in the quark level, which are usually called flavor-changing-neutral-current (FCNC) processes. In the Standard Model (SM), B meson rare decays may provide a quantitative way to determine the CKM matrix elements V_{td}, V_{ts} and V_{tb}. In the SM, FCNC transitions are forbidden at tree level. They can be induced only starting at 1-loop order, which makes their rates for decaying be sensitive to probe new physics. For these reasons, they have long been hot subjects in both experimental and theoretical studies.

Nevertheless, one remains facing difficulties in studying exclusive B meson rare decays due to the requirment of explicit calculations for the relevant form factors which involve in long distance ingredients that can not be calculated via QCD perturbative theory. Some reasonable nonperturbative methods, such as QCD sum rules, lattice simulations and phenomenological models, have been developped to estimate the long distance effects.

The rare decays have been studied by using light cone sum rules (LCSR) in full QCD theory [1,2,3,4]. As B meson can be treated as a heavy meson containing a single heavy quark, it is of interest to apply for the heavy quark effective field theory (HQEFT) to deal with the B meson rare decays. In this paper, we shall use the framework and normalization derived in Refs. [5,6,7,8], which has been applied in Refs. [9,10] to investigate the exclusive semileptionic B decays into π and ρ by using the LCSR method and obtained quite reasonable results. A more general study on exclusive semileptonic decays of heavy to light mesons within the framework of HQEFT has recently been carried out in [11]. Note that as we only keep to the leading order contributions in the expansion of $1/m_Q$, the results and conclusions are actually independent of any framework of effective field theory of heavy quarks.

We shall focus on in this paper the LCSR calculations of the form factors for the exclusive B meson rare decays $B \to K^*\gamma$ and $B \to K(K^*)\bar{l}l$ within the framework of HQEFT. In section II, we first present the hadronic matrix elements in the framework of HQEFT and derive a set of formulae for the relevant form factors. In section III, LCSR approach is applied to the relevant correlator functions in HQEFT. We then obtain four interesting relations among semileptonic type form factors and penguin type ones. Of interest, these relations are found to hold in whole momentum transfer region in the infinite mass limit of heavy quark or at the leading order of $1/m_Q$ expansion in HQEFT. Obviously, at zero recoil of the final light meson, these relations recover the so-called Isgur-Wise relations [12]. In early time, the Isgur-Wise relations were conjectured to be also valid in the region of large recoil in ref. [13]. Late on, these relations were really shown in the quark model [14,15] to hold at large recoil. In particular, one of the relations concerning the form factor in radiative decays was shown to hold in the whole momentum transfer by using QCD sum rule approach [16]. Numerical analysis of form factors is presented in section IV. Recently, one developed the so-called large energy effective theory (LEET) in which more relations were obtained near large recoil due to additional symmetries in large energy limit [17,18], while some of the relations were found to be broken down by QCD corrections [19]. Since all relations in Ref. [17] were put forward following from the combination of heavy quark effective theory (HQET) and LEET and moreover LEET is compatible with LCSR, our present method provides a reliable and important way to check the validity of LEET relations. So a detailed discussion and comparison will be presented on the basis of our HQEFT calaulation in section V. In section VI, we give the relevant branching ratios for the B meson rare decays $B \to K^*\gamma$ and $B \to K(K^*)\bar{l}l$. A brief summary is outlined in section VII.

II. GENERAL DESCRIPTION OF MATRIX ELEMENTS IN HQEFT

The transition matrix elements responsible for the B meson rare decays $B \to K^*\gamma$ and $B \to K(K^*)\bar{l}l$ may be grouped into two types: semileptonic and penguin ones. The semileptonic ones are defined as

$$\langle K(p)|\bar{s}\gamma^\mu b|B(p+q)\rangle = 2f_+(q^2)p^\mu + (f_+(q^2)+f_-(q^2))q^\mu \tag{2.1}$$

for B to K decays and

$$\begin{aligned}\langle K^*(p,\epsilon^*)|\bar{s}\gamma^\mu(1-\gamma^5)b|B(p+q)\rangle &= -i(m_B+m_{K^*})A_1(q^2)\epsilon^{*\mu}\\ &+i\frac{A_2(q^2)}{m_B+m_{K^*}}(\epsilon^*\cdot(p+q))(2p+q)^\mu + i\frac{A_3(q^2)}{m_B+m_{K^*}}(\epsilon^*\cdot(p+q))q^\mu\\ &+\frac{2V(q^2)}{m_B+m_{K^*}}\epsilon^{\mu\alpha\beta\gamma}\epsilon^*_\alpha(p+q)_\beta p_\gamma\end{aligned} \tag{2.2}$$

for B to K^* decays. In this paper, we take $\epsilon_{0123}=1$ and $\gamma^5=\gamma_5=i\gamma^0\gamma^1\gamma^2\gamma^3$.

For convenience, we may define a form factor $A_0(q^2)$ as

$$\begin{aligned}A_3(q^2) &= \frac{2(m_B+m_{K^*})m_{K^*}}{q^2}(\bar{A}_3(q^2)-A_0(q^2))\\ \bar{A}_3(q^2) &= \frac{(m_B+m_{K^*})A_1(q^2)-(m_B-m_{K^*})A_2(q^2)}{2m_{K^*}}\\ A_0(0) &= \bar{A}_3(0)\end{aligned} \tag{2.3}$$

$A_0(q^2)$ will directly enter into contributions to the relevant branching ratios.

The penguin matrix elements can be written as

$$\langle K(p)|\bar{s}\sigma^{\mu\nu}q_\nu(1+\gamma^5)b|B(p+q)\rangle = i\frac{f_T(q^2)}{m_B+m_K}\{q^2(2p+q)^\mu-(m_B^2-m_K^2)q^\mu\} \tag{2.4}$$

for B to K decays and

$$\begin{aligned}\langle K^*(p,\epsilon^*)|\bar{s}\sigma^{\mu\nu}q_\nu(1+\gamma^5)b|B(p+q)\rangle &= -i\epsilon^{\mu\alpha\beta\gamma}\epsilon^*_\alpha(p+q)_\beta p_\gamma 2T_1(q^2)\\ &+T_2(q^2)\{(m_B^2-m_{K^*}^2)\epsilon^{*\mu}-(\epsilon^*\cdot(p+q))(2p+q)^\mu\}\\ &+T_3(q^2)(\epsilon^*\cdot(p+q))\{q^\mu-\frac{q^2}{m_B^2-m_{K^*}^2}(2p+q)^\mu\}\end{aligned} \tag{2.5}$$

for B to K^* decays.

In the above definitions, p is the momentum of the light meson K or K^*. ϵ^* is the polarization vector of K^* meson, and q is the momentum transfer. $f_\pm$ and f_T are the B

to K semileptonic and penguin transition form factors respectively. A_i(i=0,1,2), V and T_i(i=1,2,3) are the corresponding ones for B to K^* transitions.

To be convenient for making Borel transformation which helps to suppress the contributions from the possible higher states of bottom mesons, we may change (2.4) and (2.5) into the following forms

$$\langle K(p)|\bar{s}\sigma^{\mu\nu}p_\nu(1+\gamma^5)b|B(p+q)\rangle = i\frac{f_T(q^2)}{m_B+m_K}\{(q\cdot p)(2p+q)^\mu - ((2p+q)\cdot p)q^\mu\} \tag{2.6}$$

$$\begin{aligned}
&\langle K^*(p,\epsilon^*)|\bar{s}\sigma^{\mu\nu}p_\nu(1+\gamma^5)b|B(p+q)\rangle = \\
&\quad -i\epsilon^{\mu\alpha\beta\gamma}\epsilon^*_\alpha(p+q)_\beta p_\gamma\{\frac{-m_B^2+m_{K^*}^2+q^2}{q^2}T_1(q^2)+\frac{m_B^2-m_{K^*}^2}{q^2}T_2(q^2)\} \\
&\quad +\epsilon^{*\mu}\{(q\cdot p)\frac{m_B^2-m_{K^*}^2}{q^2}T_2(q^2)-[(q\cdot p)\frac{m_B^2-m_{K^*}^2}{q^2}-(2p+q)\cdot p]T_1(q^2)\} \\
&\quad +q^\mu\frac{(\epsilon^*\cdot(p+q))((2p+q)\cdot p)}{m_B^2-m_{K^*}^2}\{T_3(q^2)+\frac{m_B^2-m_{K^*}^2}{q^2}(T_2(q^2)-T_1(q^2))\} \\
&\quad -(2p+q)^\mu\frac{(\epsilon^*\cdot(p+q))(q\cdot p)}{m_B^2-m_{K^*}^2}\{T_3(q^2)+\frac{m_B^2-m_{K^*}^2}{q^2}(T_2(q^2)-T_1(q^2))\}
\end{aligned} \tag{2.7}$$

When applying for the HQEFT to evaluate the matrix elements, they can be expanded into the powers of $1/m_Q$ and also be simply expressed by a set of heavy spin-flavor independent universal wave functions [6,8,9,10]. It is convenient to adopt the following normalization which relates matrix elements in full QCD with the ones in HQEFT [6]

$$\frac{1}{\sqrt{m_B}}\langle\kappa|\bar{s}\Gamma b|B\rangle = \frac{1}{\sqrt{\bar{\Lambda}_B}}\{\langle\kappa|\bar{s}\Gamma b_v|B_v\rangle + O(1/m_b)\} \tag{2.8}$$

where κ represents $K(p)$ or $K^*(p,\epsilon^*)$. The notation b_v is the effective bottom quark field. And $\bar{\Lambda}_B = m_B - m_b$ is the binding energy. From heavy quark symmetry, one can obtain the following relations [9,10,20,21,22]

$$\langle K(p)|\bar{s}\Gamma b_v|B_v\rangle = -Tr[k(v,p)\Gamma\mathcal{M}_v] \tag{2.9}$$

$$\langle K^*(p,\epsilon^*)|\bar{s}\Gamma b_v|B_v\rangle = -i\mathrm{Tr}[\Omega(v,p)\Gamma\mathcal{M}_v] \tag{2.10}$$

with

$$k(v,p) = \gamma^5[A(v\cdot p,\mu)+\hat{\not p}B(v\cdot p,\mu)] \tag{2.11}$$

$$\Omega(v,p) = L_1(v\cdot p)\not\epsilon^* + L_2(v\cdot p)(v\cdot\epsilon^*) + [L_3(v\cdot p)\not\epsilon^* + L_4(v\cdot p)(v\cdot\epsilon^*)]\hat{\not p} \tag{2.12}$$

and [6]

$$\hat{p}^\mu = \frac{p^\mu}{v\cdot p} \tag{2.13}$$

$$\mathcal{M}_v = -\sqrt{\bar{\Lambda}}\frac{1+\not v}{2}\gamma^5 \tag{2.14}$$

Where A, B and $L_i (i = 1, 2, 3, 4)$ are the leading order wave functions characterizing the heavy to light transition matrix elements in the effective field theory. $\mathcal{M}_v$ is the spin wave function associated with the heavy meson state. The vector v^μ is the four-velocity of B meson satisfying $v^2 = 1$, and $\bar{\Lambda}$ is the heavy flavor independent binding energy

$$\bar{\Lambda} = \lim_{m_Q \to \infty} \bar{\Lambda}_B$$

which reflects only the effects arising from the light degrees of freedom in the heavy B meson.

With eqs.(2.1-2.14), one arrives at the following expressions for the form factors

$$f_\pm(q^2) = \frac{1}{m_B}\sqrt{\frac{m_B\bar{\Lambda}}{\bar{\Lambda}_B}}\{A(v\cdot p) \pm B(v\cdot p)\frac{m_B}{v\cdot p}\} + \cdots \tag{2.15}$$

$$f_T(q^2) = \frac{m_B + m_K}{m_B}\sqrt{\frac{m_B\bar{\Lambda}}{\bar{\Lambda}_B}}\frac{B'(v\cdot p)}{v\cdot p} + \cdots \tag{2.16}$$

$$A_1(q^2) = \frac{2}{m_B + m_{k^*}}\sqrt{\frac{m_B\bar{\Lambda}}{\bar{\Lambda}_B}}\{L_1(v\cdot p) + L_3(v\cdot p)\} + \cdots \tag{2.17}$$

$$A_2(q^2) = 2(m_B + m_{K^*})\sqrt{\frac{m_B\bar{\Lambda}}{\bar{\Lambda}_B}}\{\frac{L_2(v\cdot p)}{2m_B^2} + \frac{L_3(v\cdot p) - L_4(v\cdot p)}{2m_B(v\cdot p)}\} + \cdots \tag{2.18}$$

$$A_3(q^2) = 2(m_B + m_{K^*})\sqrt{\frac{m_B\bar{\Lambda}}{\bar{\Lambda}_B}}\{\frac{L_2(v\cdot p)}{2m_B^2} - \frac{L_3(v\cdot p) - L_4(v\cdot p)}{2m_B(v\cdot p)}\} + \cdots \tag{2.19}$$

$$V(q^2) = \sqrt{\frac{m_B\bar{\Lambda}}{\bar{\Lambda}_B}}\frac{m_B + m_{K^*}}{m_B(v\cdot p)}L_3(v\cdot p) + \cdots \tag{2.20}$$

$$T_1(q^2) = \sqrt{\frac{m_B\bar{\Lambda}}{\bar{\Lambda}_B}}\{\frac{L'_1(v\cdot p)}{m_B} + \frac{L'_3(v\cdot p)}{v\cdot p}\} + \cdots \tag{2.21}$$

$$T_2(q^2) = 2\sqrt{\frac{m_B\bar{\Lambda}}{\bar{\Lambda}_B}}\frac{1}{m_B^2 - m_{K^*}^2}\{(m_B - v\cdot p)L'_1(v\cdot p) + \frac{m_B v\cdot p - m_{K^*}^2}{v\cdot p}L'_3(v\cdot p)\} + \cdots \tag{2.22}$$

$$T_3(q^2) = \sqrt{\frac{m_B\bar{\Lambda}}{\bar{\Lambda}_B}}\{-\frac{L'_1(v\cdot p)}{m_B} + \frac{L'_3(v\cdot p)}{v\cdot p} - \frac{m_B^2 - m_{K^*}^2}{m_B^2 v\cdot p}L'_4(v\cdot p)\} + \cdots \tag{2.23}$$

with

$$y \equiv v\cdot p = \frac{m_B^2 + m_\kappa^2 - q^2}{2m_B} \tag{2.24}$$

denoting the energy of the final light meson.

In the above formulae the dots denote possible higher order $1/m_Q$ contributions that are neglected in this paper. $B'(v\cdot p)$ and $L'_i(v\cdot p)$ are in general different from $B(v\cdot p)$ and $L_i(v\cdot p)(i = 1, 2, 3, 4)$ as they arise from different matrix elements.

III. LIGHT-CONE SUM RULES IN HQEFT

In order to calculate the relevant hadronic matrix elements which contain nonperturbative contributions and thus make QCD perturbative method lose its power, we shall apply for LCSR approach. In LCSR calculation, the relevant correlation functions are expanded near the light cone. The light cone distribution functions are introduced to describe the nonperturbative effects. In searching for reasonable and stable results, the quark-hadron duality and Borel transformation are generally adopted (for a detailed review, one may find in Refs. [23,24,26]).

The theoretical calculations can often show a simpler process in the framework of HQEFT than in QCD, which can explicitly be seen in Refs. [9,10] where the semileptonic form factors for $B \to \pi$ and ρ have been evaluated. We may directly adopt the formulae in [9,10,11] to $B \to K$ transitions by simply changing the relevant quantities corresponding to the K meson

$$A(y) = -\frac{f_K}{4Fy}\int_0^{s_0} ds e^{\frac{2\bar{\Lambda}_B - s}{T}} \left[\frac{1}{y}\frac{\partial}{\partial u} g_2(u) - \mu_K \phi_p(u) - \frac{\mu_K}{6}\frac{\partial}{\partial u}\phi_\sigma(u)\right]_{u=1-\frac{s}{2y}} \tag{3.1}$$

$$B(y) = -\frac{f_K}{4F}\int_0^{s_0} ds e^{\frac{2\bar{\Lambda}_B - s}{T}} \left[-\phi_K(u) + \frac{1}{y^2}\frac{\partial^2}{\partial u^2} g_1(u) - \frac{1}{y^2}\frac{\partial}{\partial u} g_2(u) + \frac{\mu_K}{6y}\frac{\partial}{\partial u}\phi_\sigma(u)\right]_{u=1-\frac{s}{2y}} \tag{3.2}$$

As for the B to vector Kaon meson decays, we may just adopt the definitions of K^* meson distribution functions given in [27].

$$\begin{aligned}
\langle K^*(p,\epsilon^*)|\bar{s}(-x)\sigma_{\mu\nu}d(x)|0\rangle &= -if^T_{K^*}[(\epsilon^*_\mu p_\nu - \epsilon^*_\nu p_\mu)\int_0^1 du e^{-i\xi p\cdot x}(\phi_\perp(u) + \frac{m^2_{K^*}x^2}{4}A_T(u)) \\
&+ (p_\mu x_\nu - p_\nu x_\mu)\frac{\epsilon^*\cdot x}{(p\cdot x)^2} m^2_{K^*}\int_0^1 du e^{-i\xi p\cdot x}B_T(u) + \frac{1}{2}(\epsilon^*_\mu x_\nu \\
&- \epsilon^*_\nu x_\mu)\frac{m^2_{K^*}}{p\cdot x}\int_0^1 du e^{-i\xi p\cdot x}C_T(u)]
\end{aligned} \tag{3.3}$$

$$\begin{aligned}
\langle K^*(p,\epsilon^*)|\bar{s}(-x)\gamma_\mu d(x)|0\rangle &= f_{K^*}m_{K^*}[p_\mu\frac{\epsilon^*\cdot x}{p\cdot x}\int_0^1 du e^{-i\xi p\cdot x}(\phi_\parallel(u) + \frac{m^2_{K^*}x^2}{4}A(u)) \\
&+ (\epsilon^*_\mu - p_\mu\frac{\epsilon^*\cdot x}{p\cdot x})\int_0^1 du e^{-i\xi p\cdot x} g^{(v)}_\perp(u) \\
&- \frac{1}{2}x_\mu\frac{\epsilon^*\cdot x}{(p\cdot x)^2}m^2_{K^*}\int_0^1 du e^{-i\xi p\cdot x}C(u)]
\end{aligned} \tag{3.4}$$

$$\langle K^*(p,\epsilon^*)|\bar{s}(-x)\gamma_\mu\gamma_5 d(x)|0\rangle = \frac{1}{2}(f_{K^*} - f^T_{K^*}\frac{m_s + m_d}{m_{K^*}})m_{K^*}\epsilon_{\mu\nu\alpha\beta}\epsilon^{*\nu}p^\alpha x^\beta\int_0^1 du e^{-i\xi p\cdot x} g^{(a)}_\perp(u) \tag{3.5}$$

$$\langle K^*(p,\epsilon^*)|\bar{s}(-x)d(x)|0\rangle = i(f^T_{K^*} - f_{K^*}\frac{m_s + m_d}{m_{K^*}})m^2_{K^*}(\epsilon^*\cdot x)\int_0^1 du e^{-i\xi p\cdot x} h^{(s)}_\parallel(u) \tag{3.6}$$

with $\xi = 2u - 1$. In the above definitions $\phi_\perp(u)$ and $\phi_\parallel(u)$ give the leading twist two distributions in the fraction of total momentum carried by quarks in the transversely and longitudinally polarized meson respectively. The functions $g^{(v)}_\perp(u)$ and $g^{(a)}_\parallel(u)$, which describe transverse polarizations of quarks in the longitudinally polarized meson, provide contributions of twist three. $h^{(s)}_\parallel$ is also twist three function. $A(u)$, $A_T(u)$ and $C(u)$ are twist four, while $B_T(u)$ and $C_T(u)$ are mixing twist functions. In this paper, we only consider distribution functions from two-particle contributions.

Applying the same calculation steps as in [10], we arrive at the following results

$$\begin{aligned}
L_1(y) = {} & \frac{1}{4F} e^{2\bar{\Lambda}_B/T} \int_0^{s_0} ds e^{-s/T} \frac{1}{y} \Big[f_{K^*} m_{K^*} g_\perp^{(v)}(u) \\
& + \frac{1}{4}(f_{K^*} - f_{K^*}^T \frac{m_s + m_d}{m_{K^*}}) m_{K^*} \frac{\partial}{\partial u} g_\perp^{(a)}(u) + \frac{f_{K^*}^T m_{K^*}^2}{2y} C_T(u) \Big]_{u=1-\frac{s}{2y}} \qquad (3.7) \\
L_2(y) = {} & \frac{1}{4F} e^{2\bar{\Lambda}_B/T} \int_0^{s_0} ds e^{-s/T} \Big[\frac{f_{K^*}^T m_{K^*}^2}{y^2} (\frac{1}{2} C_T(u) + B_T(u) + \frac{1}{2} \frac{\partial}{\partial u} h_\parallel^{(s)}(u)) \\
& + f_{K^*} m_{K^*}^2 (\frac{m_{K^*}}{2y^3} C(u) - \frac{m_s + m_d}{2y^2 m_{K^*}} \frac{\partial}{\partial u} h_\parallel^{(s)}(u)) \Big]_{u=1-\frac{s}{2y}} \qquad (3.8) \\
L_3(y) = {} & \frac{1}{4F} e^{2\bar{\Lambda}_B/T} \int_0^{s_0} ds e^{-s/T} \Big[-\frac{1}{4y}(f_{K^*} - f_{K^*}^T \frac{m_s + m_d}{m_{K^*}}) m_{K^*} (\frac{\partial}{\partial u} g_\perp^{(a)}(u)) \\
& + f_{K^*}^T (\phi_\perp(u) - \frac{m_{K^*}^2}{16y^2} \frac{\partial^2}{\partial u^2} A_T(u)) \Big]_{u=1-\frac{s}{2y}} \qquad (3.9) \\
L_4(y) = {} & \frac{1}{4F} e^{2\bar{\Lambda}_B/T} \int_0^{s_0} ds e^{-s/T} \frac{1}{y} \\
& \Big[f_{K^*} m_{K^*} (\phi_\parallel(u) - g_\perp^{(v)}(u) - \frac{1}{4} \frac{\partial}{\partial u} g_\perp^{(a)}(u) - \frac{m_{K^*}^2}{16y^2} \frac{\partial^2}{\partial u^2} A(u)) \\
& + \frac{f_{K^*}^T m_{K^*}^2}{y} B_T(u) + \frac{1}{4} f_{K^*}^T (m_s + m_d) \frac{\partial}{\partial u} g_\perp^{(a)}(u) \Big]_{u=1-\frac{s}{2y}} \qquad (3.10)
\end{aligned}$$

For the penguin matrix elements, we begin with considering the following correlations

$$P_T^\mu(p,q) = i \int d^4x e^{iq\cdot x} \langle K(p) | T\{ \bar{s}(x) \sigma^{\mu\nu} p_\nu (1+\gamma^5) b(x), \bar{b}(0) i\gamma^5 d(0) \} | 0 \rangle \qquad (3.11)$$

$$V_T^\mu(p,q) = i \int d^4x e^{-ip_B\cdot x} \langle K^*(p,\epsilon^*) | T\{ \bar{s}(0) \sigma^{\mu\nu} p_\nu (1+\gamma^5) b(0), \bar{b}(x) i\gamma^5 d(x) \} | 0 \rangle \qquad (3.12)$$

where $p_B = p + q$.

Making the procedures similar to Refs. [9,10], one can easily derive the explicit expressions for $B'(y)$ and $L_i'(y)$, which are exactly the same as $B(y)$ and $L_i(y)$ in (3.2) and (3.7-3.10) at the leading order of $1/m_Q$ expansion. From (2.15) to (2.23), we obtain the following four interesting relations among the semileptonic type and penguin type form factors.

$$f_T(q^2) = \frac{m_B + m_K}{2m_B} (f_+(q^2) - f_-(q^2)) \qquad (3.13)$$

$$T_1(q^2) = \frac{m_B^2 - m_{K^*}^2 + q^2}{2m_B} \frac{V(q^2)}{m_B + m_{K^*}} + \frac{m_B + m_{K^*}}{2m_B} A_1(q^2) \qquad (3.14)$$

$$T_2(q^2) = \frac{2}{m_B^2 - m_{K^*}^2} [\frac{(m_B - y)(m_B + m_{K^*})}{2} A_1(q^2) + \frac{m_B(y^2 - m_{K^*}^2)}{m_B + m_{K^*}} V(q^2)] \qquad (3.15)$$

$$T_3(q^2) = \frac{m_B^2 - m_{K^*}^2}{m_B q^2} m_{K^*} A_0(q^2) - \frac{m_B^2 - m_{K^*}^2 + q^2}{2m_B q^2} [(m_B + m_{K^*}) A_1(q^2) - (m_B - m_{K^*}) A_2(q^2)]$$

$$+\frac{m_B^2+3m_{K^*}^2-q^2}{2m_B(m_B+m_{K^*})}V(q^2) \tag{3.16}$$

Note that these relations hold in the whole momentum transfer region. In fact, they can simply be obtained from eqs.(2.9) and (2.10) by assuming that the light meson wave functions $k(v,p)$ and $\Omega(v,p)$ are universal for different types of the currents, namely they are independent of the choice of Γ in the currents. The second relation was actually observed in ref. [16] by using QCD sum rule approach.

In the heavy quark limit near zero recoil point ($q^2 \to q^2_{max}$), the above relations were known as Isgur-Wise relations [12]. In Refs. [27,28], some detailed discussions were made to explore the Isgur-Wise relations in both small and large recoil conditions by using full LCSR method, where it was shown that the Isgur-Wise relations are satisfied very well at $q^2 \to 0$ (large recoil) and hold with about 80% accuracy at large q^2. In Ref. [29], conclusions were made that the Isgur-Wise relations are valid up to 70% in the whole q^2 region by applying for the three point QCD sum rules method. In the quark model, the authors of Refs. [14,15] concluded that Isgur-Wise relations also hold at large recoil.

In here we have further confirmed the existed analyzes in the literature and arrived at a general conclusion that the relations (3.13-3.16) hold for whole allowed region of momentum transfer q^2 at the leading order of $1/m_Q$ expansion, which has nothing to do with the energy of the final light meson. This may provide a more general proof in support of the hypothesis made in the early time by the authors in Ref. [13]. As a consequence, it becomes remarkable that one can directly read off the penguin form factors f_T and $T_i (i = 1,2,3)$ from the relations in eqs. (3.13-3.16) without the tedious calculations from LCSR to Borel transformation. In Ref. [11], we have shown that when applying the HQEFT to heavy to light semileptonic decays, heavy quark expansion and heavy quark symmetry enable us to relate various decay channels, consequently, the theoretical analysis is much simplified and the number of independent functions is greatly abated though the number of independent functions in a single decay channel does not decrease. Here with the four exact relations, the number of independent variables among the form factors $f_\pm$ and f_T is straightforwardly reduced to two. The number of independent variables in the rare decay $B \to K^* l\bar{l}$ is then reduced from seven form factors to four form factors. One sees that for the B meson rare decays the heavy quark expansion exhibits its more powerful advantages, the number of independent functions is found to be largely reduced even in a single decay channel.

IV. NUMERICAL ANALYSIS AND RESULTS FOR FORM FACTORS

The light cone wave functions play an important role for a precise calculation of form factors. They have been studied by several groups. We shall use the results given in [24,30,31,32] for K and the ones in [27] for K^* meson in our following analyses. The asymptotic form and the scale dependence of them are taken from perturbative QCD calculations given in [33,34].

We shall first present all two-particle light cone amplitudes of Kaon appearing in (3.1) and (3.2)

$$\phi_K(u,\mu) = 6u(1-u)\Big[1 + a_1(\mu)(3(2u-1)) + a_2(\mu)(\frac{15}{2}(2u-1)^2 - \frac{3}{2})$$

$$
\begin{aligned}
&\qquad +a_3(\mu)(\frac{35}{2}(2u-1)^3-\frac{15}{2}(2u-1))+a_4(\mu)\frac{15}{8}(21(2u-1)^4-14(2u-1)^2+1)\Big] \\
\phi_p(u,\mu) &= 1+\frac{1}{2}B_2(\mu)[3(2u-1)^2-1]+\frac{1}{8}B_4(\mu)[35(2u-1)^4-30(2u-1)^2+3] \\
\phi_\sigma(u,\mu) &= 6u(1-u)\{1+\frac{3}{2}C_2(\mu)[5(2u-1)^2-1]+\frac{15}{8}C_4(\mu)[21(2u-1)^4-14(2u-1)^2+1]\} \\
g_1(u,\mu) &= \frac{5}{2}\delta^2(\mu)u^2(1-u)^2+\frac{1}{2}\epsilon(\mu)\delta^2(\mu)\Big[u(1-u)(2+13u(1-u)+10u^3(\log u)(2-3u+\frac{6}{5}u^2) \\
&\qquad +10(1-u)^3(\log(1-u))(2-3(1-u)+\frac{6}{5}(1-u)^2))\Big] \\
g_2(u,\mu) &= \frac{10}{3}\delta^2(\mu)u(1-u)(2u-1) \qquad (4.1)
\end{aligned}
$$

For the relevant parameters, we will take the following values in our numerical calculations

$$
\begin{gathered}
a_1(\mu_b)=0.15,\;\; a_2(\mu_b)=0.16,\;\; a_3(\mu_b)=0.05,\;\; a_4(\mu_b)=0.06, \\
B_2(\mu_b)=0.29,\;\; B_4(\mu_b)=0.58,\;\; C_2(\mu_b)=0.059,\;\; C_4(\mu_b)=0.034, \\
\delta^2(\mu_b)=0.17\mathrm{GeV}^2,\;\; \epsilon(\mu_b)=0.36 \qquad (4.2)
\end{gathered}
$$

where we choose $\mu_b=\sqrt{m_B^2-m_b^2}\approx 2.4\mathrm{GeV}$ which is the appropriate scale characterizing the typical virtuality of the b quark. The SU(3) flavor violation effects of Kaon has been taken into account in $\phi_K(u,\mu)$ with non-vanishing coefficients $a_1(\mu_b)$ and $a_3(\mu_b)$. The SU(3) flavor breaking effects in the higher twist amplitudes are neglected in this paper as they only have a small contribution [35].

For the light vector K^* meson wave functions, we use the expressions given in [27]. The light meson SU(3) flavor breaking effects are taken into account in the leading twist distributions and partially in the twist three, but ignored in twist four.

Other parameters needed are listed in the following :

$$
\begin{gathered}
m_B=5.28\mathrm{GeV},\;\; m_b=4.75\mathrm{GeV},\;\; m_K=0.49\mathrm{GeV},\;\; m_{K^*}=0.89\mathrm{GeV}, \\
\bar\Lambda_B=0.53\mathrm{GeV},\;\; \bar\Lambda=(0.53\pm0.08)\mathrm{GeV},\;\; F=(0.30\pm0.06)\mathrm{GeV}^{3/2}, \\
f_K=0.16\mathrm{GeV},\;\; f_{K^*}=(226\pm28)\mathrm{MeV},\;\; f_{K^*}^{\perp}(\mu_b)=(175\pm9)\mathrm{MeV}, \\
\mu_K(\mu_b)=\tfrac{m_K^2}{m_s+m_{u,d}}\approx 2.02\mathrm{GeV} \qquad (4.3)
\end{gathered}
$$

As for the parameters s_0 and T, according to LCSR criterion that the contributions from both the higher states and higher twist four distribution functions should not be larger than 30%. Thus we choose the region for T to be $1\mathrm{GeV} < T < 3\mathrm{GeV}$. In this region the curves of $f_\pm$ and f_T for B to K transitions and $A_i(i=0,1,2)$, V and $T_i(i=1,2,3)$ for B to K^* transitions become most stable at the threshold energy $s_0=2.1-2.7(2.4\pm0.3)\mathrm{GeV}$ and $s_0=1.8-2.4(2.1\pm0.3)\mathrm{GeV}$ respectively, which may be seen explicitly from Fig.1 to Fig.10.

It is known that the light cone expansion and the sum rule method may be broken down at large momentum transfer (practically as q^2 approaches near half of m_b^2) [24], which may be seen explicitly from Fig.11-20. Where the curves of form factors calculated from LCSR likely become unstable at large q^2 region. Thus for the behavior of the form factors in the whole kinematically accessible region, we may use the following parametrization for the transfer momentum dependence of the form factors

$$F(q^2) = \frac{F(0)}{1 - a_F q^2/m_B^2 + b_F (q^2/m_B^2)^2} \tag{4.4}$$

where $F(q^2)$ can be any of the form factors f_+, f_-, f_T, $A_i (i = 0, 1, 2)$, V and $T_i (i = 1, 2, 3)$. We directly use LCSR predictions to fit the parameters. This is because K^* and K mesons contain a relative heavy strange quark (in comparison with the u and d quarks), so that they are comparatively heavy and shorten the kinematically allowed ranges of B to K^* and K decays in comparison with the ranges for B to π decays. Therefore the sum rules are expected to yield reasonable values for most allowed region of q^2 in the K^* and K meson cases.

With the above analyses, we are then able to fix the three parameters for each form factor. We plot in Fig.11-20 the form factors as functions of q^2 with different threshold energy $s_0 = 2.1, 2.4, 2.7$GeV for B to K transitions and $s_0 = 1.8, 2.1, 2.4$GeV for B to K^* transitions at $T = 2.0$GeV. Our numerical results of form factors at $q^2 = 0$ are given in Table 1, where the uncertainties of the form factors arise from the uncertainties of the threshold energy s_0, the Borel parameter T and the parameters in (4.3). In our values, the uncertainties coming from s_0 are about 10%, from T and the parameters in (4.3) are around 15%. The total uncertainties are up to 25%. For comparison, we list in table 1 the numerical results obtained from other approaches: QCD LCSR, LEET, quark model (QM), lattice, three point sum rules (SR) and PQCD calculation.

Table 1. Values for form factors of $B \to K l\bar{l}$,$B \to K^* l\bar{l}$ and $B \to K^*\gamma$ at $q^2 = 0$.

	present	LCSR [1]	LEET [36]	QM [37]	lattice [38]	lattice [39]	SR [29]	PQCD [40]
$f_+(0)$	$0.454\ ^{+0.053}_{-0.075}$	$0.319\ ^{+0.052}_{-0.041}$	$---$	0.36	$---$	0.30(4)	0.25	$---$
$f_0(0)$	$0.454\ ^{+0.053}_{-0.075}$	$0.319\ ^{+0.052}_{-0.041}$	$---$	0.36	$---$	0.30(4)	0.25	$---$
$f_T(0)$	$0.447\ ^{+0.046}_{-0.069}$	$0.355\ ^{+0.016}_{-0.055}$	$---$	0.35	$---$	0.29(6)	0.14	$---$
$A_0(0)$	$0.468\ ^{+0.082}_{-0.112}$	$0.471\ ^{+0.127}_{-0.059}$	$---$	0.45	0.32	$---$	0.30	0.407
$A_1(0)$	$0.350\ ^{+0.068}_{-0.089}$	$0.337\ ^{+0.048}_{-0.043}$	0.27 ± 0.03	0.36	0.28	$---$	0.37	0.266
$A_2(0)$	$0.302\ ^{+0.063}_{-0.080}$	$0.282\ ^{+0.038}_{-0.036}$	$---$	0.32	$---$	$---$	0.40	0.202
$V(0)$	$0.426\ ^{+0.070}_{-0.098}$	$0.457\ ^{+0.091}_{-0.058}$	0.36 ± 0.04	0.44	0.38	$---$	0.47	0.355
$T_1(0)$	$0.382\ ^{+0.068}_{-0.093}$	$0.379\ ^{+0.058}_{-0.045}$	0.31 ± 0.02	0.39	0.32	$---$	0.38	0.315
$T_2(0)$	$0.382\ ^{+0.068}_{-0.093}$	$0.379\ ^{+0.058}_{-0.045}$	$---$	0.39	0.32	$---$	0.38	0.315
$T_3(0)$	$0.266\ ^{+0.045}_{-0.063}$	$0.260\ ^{+0.035}_{-0.016}$	$---$	0.27		$---$	1.4	0.207

V. ON VALIDITY OF RELATIONS IN LEET

Recently, it was noted in Ref. [17] that by applying HQET to the initial heavy meson and meanwhile adopting LEET to describe the final light meson, more relations were obtained at the leading order of heavy quark mass and large energy expansion. Eventually, the total number of independent form factors is reduced to three near the large recoil point. While those symmetry relations were shown [19] to be broken down when radiative corrections are considered. The contributions of the second order in the ratio of the light meson mass to the large recoil energy were taken into account in Ref. [18].

To compare our results with those in Ref. [17] and also to see how much accuracy of the large energy effective theory would be, we first introduce the following definitions

$$\zeta(m_B, y) = \sqrt{\frac{m_B\bar{\Lambda}}{\bar{\Lambda}_B}}\frac{1}{y}B(y) \tag{5.1}$$

$$\zeta_A(m_B, y) = \sqrt{\frac{m_B\bar{\Lambda}}{\bar{\Lambda}_B}}\frac{1}{m_B}A(y) \tag{5.2}$$

$$\zeta_\parallel(m_B, y) = \sqrt{\frac{m_B\bar{\Lambda}}{\bar{\Lambda}_B}}(\frac{1}{m_{K^*}}L_4(y) - \frac{y}{m_B m_{K^*}}L_2(y)) \tag{5.3}$$

$$\zeta_\perp(m_B, y) = \sqrt{\frac{m_B\bar{\Lambda}}{\bar{\Lambda}_B}}\frac{L_3(y)}{y} \tag{5.4}$$

$$\zeta_1(m_B, y) = \sqrt{\frac{m_B\bar{\Lambda}}{\bar{\Lambda}_B}}\frac{L_1(y)}{y} \tag{5.5}$$

$$\zeta_2(m_B, y) = \sqrt{\frac{m_B\bar{\Lambda}}{\bar{\Lambda}_B}}\frac{y}{m_B m_{K^*}}L_2(y) \tag{5.6}$$

With these functions, the form factors in eqs.(2.15-2.23) can be expressed as

$$f_\pm(q^2) = \zeta_A(m_B, y) \pm \zeta(m_B, y) \tag{5.7}$$

$$\begin{aligned} f_0(q^2) &\equiv \frac{q^2}{m_B^2 - m_K^2}f_-(q^2) + f_+(q^2) \\ &= (1 - \frac{q^2}{m_B^2 - m_K^2})\zeta(m_B, y) + (1 + \frac{q^2}{m_B^2 - m_K^2})\zeta_A(m_B, y) \end{aligned} \tag{5.8}$$

$$f_T(q^2) = (1 + \frac{m_K}{m_B})\zeta(m_B, y) \tag{5.9}$$

$$A_0(q^2) = (1 - \frac{m_{K^*}^2}{ym_B})\zeta_\parallel(m_B, y) + \frac{m_{K^*}}{m_B}\zeta_\perp + \frac{y}{m_{K^*}}\zeta_1(m_B, y) - \frac{q^2}{ym_B}\zeta_2(m_B, y) \tag{5.10}$$

$$A_1(q^2) = \frac{2y}{m_B + m_{K^*}}(\zeta_\perp(m_B, y) + \zeta_1(m_B, y)) \tag{5.11}$$

$$A_2(q^2) = (1 + \frac{m_{K^*}}{m_B})(\zeta_\perp(m_B, y) - \frac{m_{K^*}}{y}\zeta_\parallel(m_B, y)) \tag{5.12}$$

$$V(q^2) = (1 + \frac{m_{K^*}}{m_B})\zeta_\perp(m_B, y) \tag{5.13}$$

$$T_1(q^2) = \zeta_\perp(m_B, y) + \frac{y}{m_B}\zeta_1(m_B, y) \tag{5.14}$$

$$T_2(q^2) = (1 - \frac{q^2}{m_B^2 - m_{K^*}^2})\zeta_\perp(m_B, y) + (1 + \frac{q^2}{m_B^2 - m_{K^*}^2})\frac{y}{m_B}\zeta_1(m_B, y) \tag{5.15}$$

$$T_3(q^2) = \zeta_\perp(m_B, y) - (1 - \frac{m_{K^*}^2}{m_{m_B}^2})\frac{m_{K^*}}{y}(\zeta_\parallel(m_B, y) + \zeta_2(m_B, y)) - \frac{y}{m_B}\zeta_1(m_B, y) \tag{5.16}$$

Comparing the above forms with the ones given by eqs.(104)-(113) in Ref. [17], it is obvious that the three functions $\zeta_A(q^2)$, $\zeta_1(q^2)$ and $\zeta_2(q^2)$ should vanish, i.e., $\zeta_A(q^2) = \zeta_1(q^2) = \zeta_2(q^2) = 0$, in order to reproduce the results in LEET. For a quantitative comparison, we plot in Fig.21 three curves $\zeta_\parallel(q^2)$, $\zeta_\perp(q^2)$ and $\zeta(q^2)$ as functions of momentum transfer q^2, and in Fig.22 the three ratios $\zeta_2(q^2)/\zeta_\parallel(q^2)$, $\zeta_1(q^2)/\zeta_\perp(q^2)$ and $\zeta_A(q^2)/\zeta(q^2)$ as functions of q^2. It is seen that the three functions $\zeta_A(q^2)$, $\zeta_1(q^2)$ and $\zeta_2(q^2)$ do have small but sizable contributions relative to the three nonzero functions $\zeta_\parallel(q^2)$, $\zeta_\perp(q^2)$ and $\zeta(q^2)$ in LEET. Numerically, they are about 20%, 10% and 10% respectively when $q^2 = 0$. For the ratios $\zeta_2(q^2)/\zeta_\parallel(q^2)$ and $\zeta_A(q^2)/\zeta(q^2)$, they are almost independent of the momentum transfer q^2. For the ratio $\zeta_1(q^2)/\zeta_\perp(q^2)$, it ranges from 10% to 40% as q^2 increases.

To be more clear, we directly plot in Figs.23-29 the ratios between the form factors, i.e., $F_{iLEET}(q^2)/F_i(q^2)$ at center value of s_0 with $T = 2.0$GeV. Here $F_{iLEET}(q^2)$ denote the form factors obtained from HQET/LEET relations, namely $\zeta_A(q^2) = \zeta_1(q^2) = \zeta_2(q^2) = 0$, and $F_i(q^2)$s are the form factors obtained in present paper, namely the three functions $\zeta_A(q^2)$, $\zeta_1(q^2)$ and $\zeta_2(q^2)$ are not zero and given in eq. (5.2), (5.5) and (5.6). It is seen that, except the ratio $A_{0LEET}/A_0 \approx 0.78$, the other ratios near large recoil point ($q^2 \to 0$) have the value $F_{iLEET}/F_i = 0.9 \sim 1.0$. More explicitly speaking $f_{+LEET}/f_+ \approx f_{TLEET}/f_T \approx 0.9$, $A_{1LEET}/A_1 \approx 0.92$, $T_{1LEET} \approx T_{2LEET}/T_2 \approx 0.96$ and $T_{3LEET}/T_3 \approx 0.98$. So we can say the form factors F_{iLEET} have the accuracy beter than 90% as comparation with F_i except A_{0LEET} whose accuracy is only about 78%. This exception can be explained as that the third term on the R.H.S. of the equation (5.10) contains the factor y/m_{K^*}, which undoubtedly enhances several times the contribution of $\zeta_1(q^2)$ when $q^2 = 0$. So when B decays to more light final mesons, say ρ, the LEET relation for $A_0(q^2)$ will work worse. It is particularly noted that ratios f_{+LEET}/f_+, T_{1LEET}/T_1 and T_{3LEET}/T_3, which take value among the area $0.85 \sim 0.90$, $0.91 \sim 0.95$ and $1.0 \sim 1.05$ respectively in the whole q^2, are almost independent of q^2. The reason is clear since the ratios $\zeta_A(q^2)/\zeta(q^2)$ in (5.7) and $\zeta_2(q^2)/\zeta_\parallel(q^2)$ in (5.16) are almost independent of the momentum transfer q^2 and the coefficient of the wave function $\zeta_1(m_B, y)$ is associated with the factors y/m_B in (5.14) and (5.16), which have a tendency to suppress the contribution of $\zeta_1(m_B, y)$ as q^2 increases. While the other ratios, especially the ratio A_{0LEET}/A_0, get worse results for large q^2, say $q^2 \approx 15GeV^2$, which can be considered as far from large recoil. For instance A_{0LEET} is only about half of A_0 at $q^2 \approx 15GeV^2$. This means that LEET becomes not appropriate for large q^2 region. The reason lies in that on one hand $\zeta_1(q^2)/\zeta_\perp(q^2)$ counts notablly when q^2 is large. On the other hand, in the general form factor formulations (5.8), (5.10) and (5.15), there is a factor q^2 to enhance the contributions of $\zeta_A(q^2)$, $\zeta_2(q^2)$ and $\zeta_1(q^2)$ when q^2 increases. In addition, as can be seen from (5.9), (5.12) and (5.13), f_{TLEET}, A_{2LEET} and V_{LEET} are same as the corresponding one obtained by HQEFT in present paper.

Besides the relations (3.13-3.16), LEET leads to three additional relations [17]

$$f_T(q^2) = (1 + \frac{m_K}{m_B}) f_+(q^2) \tag{5.17}$$

$$A_0(q^2) = (1 - \frac{m_{K^*}^2}{y m_B}) \frac{y m_B}{m_{K^*}(m_B + m_{K^*})} (V(q^2) - A_2(q^2)) + \frac{m_{K^*}(m_B + m_{K^*})}{2 y m_B} A_1(q^2) \tag{5.18}$$

$$A_1(q^2) = \frac{2 y m_B}{(m_B + m_{K^*})^2} V(q^2) \tag{5.19}$$

To check this relations, we plot in Figs.30-32 the three form factors f_T, A_0 and A_1 obtained from the direct calculations (i.e., left-hand side (LHS)) and from the relations (i.e., right-hand side (RHS)). The numerical comparison of the LHS and RHS of the above equations shows that near the large recoil point ($q^2 \to 0$) the relations (5.17) and (5.19) both hold within 90% accuracy, but the relations (5.18) only hold about 80% accuracy. In particular, the deviations of LHS and RHS in relations (5.17) and (5.19) do not exceed 20% through whole q^2, while that of relation (5.18) at best hold with 40%.

VI. RESULTS FOR BRANCHING RATIOS

The relevant branching ratios are able to be calculated with the form factors given above. The relevant decay width formulae have the following general forms [1]

$$\begin{aligned}\frac{d\Gamma}{d\hat{s}} &= \frac{G_F^2\alpha^2 m_B^5}{2^{11}\pi^5}|V_{ts}^*V_{tb}|^2\hat{u}(\hat{s})\Big\{(|A'(\hat{s})|^2+|C'(\hat{s})|^2)(\lambda(\hat{s})-\frac{\hat{u}(\hat{s})^2}{3})\\ &\quad +|C'(\hat{s})|^2 4\hat{m}_l^2(2+2\hat{m}_K^2-\hat{s})+Re(C'(\hat{s})D'(\hat{s})^*)8\hat{m}_l^2(1-\hat{m}_K^2)+|D'(\hat{s})|^2 4\hat{m}_l^2\hat{s}\Big\} \qquad (6.1)\end{aligned}$$

for $B \to K\bar{l}l$, and

$$\begin{aligned}\frac{d\Gamma}{d\hat{s}} &= \frac{G_F^2\alpha^2 m_B^5}{2^{11}\pi^5}|V_{ts}^*V_{tb}|^2\hat{u}(\hat{s})\Big\{\frac{|A(\hat{s})|^2}{3}\hat{s}\lambda(\hat{s})(1+2\frac{\hat{m}_l^2}{\hat{s}})+|E(\hat{s})|^2\hat{s}\frac{\hat{u}(\hat{s})^2}{3}\\ &\quad +\frac{1}{4\hat{m}_{K^*}^2}\Big[|B(\hat{s})|^2(\lambda(\hat{s})-\frac{\hat{u}(\hat{s})^2}{3}+8\hat{m}_{K^*}^2(\hat{s}+2\hat{m}_l^2))+|F(\hat{s})|^2(\lambda(\hat{s})-\frac{\hat{u}(\hat{s})^2}{3}+8\hat{m}_{K^*}^2(\hat{s}-4\hat{m}_l^2))\Big]\\ &\quad +\frac{\lambda(\hat{s})}{4\hat{m}_{K^*}^2}\Big[|C(\hat{s})|^2(\lambda(\hat{s})-\frac{\hat{u}(\hat{s})^2}{3})+|G(\hat{s})|^2(\lambda(\hat{s})-\frac{\hat{u}(\hat{s})^2}{3}+4\hat{m}_l^2(2+2\hat{m}_{K^*}^2-\hat{s}))\Big]\\ &\quad -\frac{1}{2\hat{m}_{K^*}^2}\Big[Re(B(\hat{s})C(\hat{s})^*)(\lambda(\hat{s})-\frac{\hat{u}(\hat{s})^2}{3})(1-\hat{m}_{K^*}^2-\hat{s})\\ &\quad +Re(F(\hat{s})G(\hat{s})^*)((\lambda(\hat{s})-\frac{\hat{u}(\hat{s})^2}{3})(1-\hat{m}_{K^*}^2-\hat{s})+4\hat{m}_l^2\lambda(\hat{s}))\Big]\\ &\quad -2\frac{\hat{m}_l^2}{\hat{m}_{K^*}^2}\lambda(\hat{s})\Big[Re(F(\hat{s})H(\hat{s})^*)-Re(G(\hat{s})H(\hat{s})^*)(1-\hat{m}_{K^*}^2)\Big]+\frac{\hat{m}_l^2}{\hat{m}_{K^*}^2}\hat{s}\lambda(\hat{s})|H(\hat{s})|^2\Big\} \qquad (6.2)\end{aligned}$$

for $B \to K^*\bar{l}l$, as well as

$$\Gamma = \frac{G_F^2\alpha m_b^2 m_B^3}{32\pi^4}|V_{ts}^*V_{tb}|^2|C_7^{eff}|^2|T_1(0)|^2(1-\hat{m}_{K^*})^3 \qquad (6.3)$$

for $B \to K^*\gamma$.

The functions appearing in the above decay width formulae are defined as [1,41]

$$A'(\hat{s}) = C_9^{eff}(\hat{s})f_+(\hat{s})+\frac{2\hat{m}_b}{1+\hat{m}_K}C_7^{eff}f_T(\hat{s}), \qquad (6.4)$$

$$B'(\hat{s}) = C_9^{eff}(\hat{s})f_-(\hat{s})-\frac{2\hat{m}_b}{\hat{s}}(1-\hat{m}_K)C_7^{eff}f_T(\hat{s}), \qquad (6.5)$$

$$C'(\hat{s}) = C_{10}f_+(\hat{s}), \qquad (6.6)$$

$$
\begin{aligned}
D'(\hat{s}) &= C_{10} f_-(\hat{s}), && (6.7)\\
A(\hat{s}) &= \frac{2}{1+\hat{m}_{K^*}} C_9^{eff}(\hat{s}) V(\hat{s}) + \frac{4\hat{m}_b}{\hat{s}} C_7^{eff} T_1(\hat{s}), && (6.8)\\
B(\hat{s}) &= (1+\hat{m}_{K^*})[C_9^{eff}(\hat{s}) A_1(\hat{s}) + \frac{2\hat{m}_b}{\hat{s}}(1-\hat{m}_{K^*}) C_7^{eff} T_2(\hat{s})], && (6.9)\\
C(\hat{s}) &= \frac{1}{1-\hat{m}_{K^*}^2}[(1-\hat{m}_{K^*}) C_9^{eff}(\hat{s}) A_2(\hat{s}) + 2\hat{m}_b C_7^{eff}(T_3(\hat{s}) + \frac{1-\hat{m}_{K^*}^2}{\hat{s}} T_2(\hat{s}))], && (6.10)\\
D(\hat{s}) &= \frac{1}{\hat{s}}[C_9^{eff}(\hat{s})((1+\hat{m}_{K^*})A_1(\hat{s}) - (1-\hat{m}_{K^*})A_2(\hat{s}) - 2\hat{m}_{K^*} A_0(\hat{s})) - 2\hat{m}_b C_7^{eff} T_3(\hat{s})], && (6.11)\\
E(\hat{s}) &= \frac{2}{1+\hat{m}_{K^*}} C_{10} V(\hat{s}), && (6.12)\\
F(\hat{s}) &= (1+\hat{m}_{K^*}) C_{10} A_1(\hat{s}), && (6.13)\\
G(\hat{s}) &= \frac{1}{1+\hat{m}_{K^*}} C_{10} A_2(\hat{s}), && (6.14)\\
H(\hat{s}) &= \frac{1}{\hat{s}} C_{10}(\hat{s})[(1+\hat{m}_{K^*})A_1(\hat{s}) - (1-\hat{m}_{K^*})A_2(\hat{s}) - 2\hat{m}_{K^*} A_0(\hat{s})], && (6.15)\\
\lambda(\hat{s}) &= 1 + \hat{m}_{K,K^*}^4 + \hat{s}^2 - 2\hat{s} - 2\hat{m}_{K,K^*}^2(1+\hat{s}), && (6.16)\\
\hat{u}(\hat{s}) &= \sqrt{\lambda(\hat{s})(1 - 4\frac{\hat{m}_l^2}{\hat{s}})}, && (6.17)\\
C_9^{eff}(\hat{s}) &= C_9 + g(\hat{m}_c, \hat{s})(3C_1 + C_2 + 3C_3 + C_4 + 3C_5 + C_6) - \frac{1}{2} g(1,\hat{s})(4C_3 + 4C_4 + 3C_5 + C_6)\\
&\quad - \frac{1}{2} g(0,\hat{s})(C_3 + 3C_4) + \frac{2}{9}(3C_3 + C_4 + 3C_5 + C_6), && (6.18)\\
g(0,\hat{s}) &= \frac{8}{27} - \frac{8}{9}\ln\frac{m_b}{\mu} - \frac{4}{9}\ln\hat{s} + \frac{4}{9} i\pi, && (6.19)\\
g(z,\hat{s}) &= \frac{8}{27} - \frac{8}{9}\ln\frac{m_b}{\mu} - \frac{8}{9}\ln z + \frac{4}{9} x\\
&\quad - \frac{2}{9}(2+x)\sqrt{|1-x|}\begin{cases} (\ln|\frac{\sqrt{1-x}+1}{\sqrt{1-x}-1}| - i\pi), & for\ \ x \equiv \frac{4z^2}{\hat{s}} < 1\\ 2\arctan\frac{1}{\sqrt{x-1}}, & for\ \ x \equiv \frac{4z^2}{\hat{s}} > 1. \end{cases} && (6.20)
\end{aligned}
$$

with $\hat{s} = \frac{q^2}{m_B^2}$,$\hat{m}_{K,K^*} = \frac{m_{K,K^*}}{m_B}$,$\hat{m}_{b,c} = \frac{m_{b,c}}{m_B}$ and $\hat{m}_l = \frac{m_l}{m_B}$. For the Wilson coefficients C_i, we take the results calculated in the naive dimensional regularization (NRD) scheme [42] and their values are listed in Table 2.

Table 2. Values of the Wilson coefficients with choosing the renormalization scale at $\mu = m_b = 4.8$GeV. Here, $C_7^{eff} = C_7 - C_5/3 - C_6$.

C_1	C_2	C_3	C_4	C_5	C_6	C_7	C_7^{eff}	C_9	C_{10}
-0.248	1.107	0.011	-0.026	0.007	-0.031	-0.342	-0.313	4.344	-4.669

It is seen that once the decay rates and the form factors are precisely determined, one is able to extract the CKM matrix elements. Here we may use the current reasonable values of CKM matrix elements extracted from other processes and unitarity of the CKM matrix to predict the branching ratios for the B meson rare decays. When taking the CKM matrix element $|V_{tb}V_{ts}| = 0.0385$, we present our results in Table 3. For comparison, we also list the results given in [1] and the ones from experimental measurements. It is seen that within the uncertainties, our prediction is consistent with the experimental results.

Table 3. Branching ratios (Br) for B rare decays in standard model (SM). In deriving the branching ratios we have used the lifetime of B meson: $\tau_B = 1.65$ps. Where the errors mainly come from the uncertainties of the threshold energy s_0, the Borel parameter T and the parameters in (4.3).

	present values	values in [1]	experiment
$B \to Ke\bar{e}$ $B \to K\mu\bar{\mu}$	$(0.84^{+0.10}_{-0.24})\times 10^{-6}$	$(0.57^{+0.16}_{-0.10})\times 10^{-6}$	$(0.75^{+0.25}_{-0.21} \pm 0.09)\times 10^{-6}$ [43]
$B \to K\tau\bar{\tau}$	$(1.73^{+0.21}_{-0.47})\times 10^{-7}$	$(1.3^{+0.3}_{-0.1})\times 10^{-7}$	$------$
$B \to K^*\gamma$	$(5.47^{+2.14}_{-2.34})\times 10^{-5}$	$(5.37^{+1.77}_{-1.20})\times 10^{-5}$ △	$(4.55^{+0.72}_{-0.68} \pm 0.34)\times 10^{-5}$ △△ [44] $(4.96\pm 0.67\pm 0.45)\times 10^{-5}$ △△ [45] $(5.7 \pm 3.3)\times 10^{-5}$ [46]
$B \to K^*e\bar{e}$	$(1.86^{+0.52}_{-0.73})\times 10^{-6}$	$(2.3^{+0.7}_{-0.4})\times 10^{-6}$	$(2.08^{+1.23+0.35}_{-1.00-0.37})\times 10^{-6}$ [43]
$B \to K^*\mu\bar{\mu}$	$(1.78^{+0.49}_{-0.70})\times 10^{-6}$	$(1.9^{+0.5}_{-0.3})\times 10^{-6}$	$------$
$B \to K^*\tau\bar{\tau}$	$(1.68^{+0.18}_{-0.55})\times 10^{-7}$	$(1.9^{+0.1}_{-0.2})\times 10^{-7}$	$------$

△ :The value is obtained through (6.3) by using the form factor $T_1(0) = 0.379^{+0.058}_{-0.045}$ presented in Ref. [1].
△△ : The value is for $B^0 \to K^{0*}\gamma$.

VII. SUMMARY

In summary, we have studied the B meson rare decays in the framework of HQEFT. The semileptonic type and penguin type form factors have been derived by using LCSR method in HQEFT. It has been seen that the heavy quark expansion brings a much simplification to B meson rare decays. Isgur-Wise relations among the semileptonic type and penguin type form factors have been proved to hold for the whole momentum transfer region at the leading order $1/m_Q$ expansion. As a consequence, all the form factors can be neatly characterized by a set of wave functions (A, B and $L_i (i = 1, 2, 3, 4)$) at the leading order of $1/m_Q$ expansion. Furthermore from our quantitative discussion, it is obvious that LEET is a valid method for heavy-to-light transition. LEET relations hold within 80% accuracy at large recoil point on the whole, and most of them even hold better than 90% accuracy. Moreover, our numerical prediction is consistent with the experimental results. We then conclude that the branching ratios of B meson rare decays can be reasonably predicted based on LCSR approach within the framework of HQEFT. Nevertheless, in order to match the expected measurements of B factories in the near future, a more accurate calculation of the form factors for the B meson rare decays is urgently required.

ACKNOWLEDGMENTS

This work was supported in part by the key projects of National Science Foundation of China (NSFC) and Chinese Academy of Sciences.

REFERENCES

[1] A. Ali, P. Ball, L. T. Handoko and G. Hiller, Phys. Rev. D **61**, 074024 (2000).

[2] T. M. Aliev, A. Özpineci, M. Savci and H. Koru, Phys. Lett. B **400**, 194 (hep-ph/9702209).

[3] T. M. Aliev, A. Özpineci and M. Savci, Phys. Rev. D **56**, 4260 (1997).

[4] A. S. Safir, EPJ C **15**, 1 (2001) (hep-ph/0109232)

[5] Y. L. Wu, Mod. Phys. Lett. A **8**, 819 (1993).

[6] W. Y. Wang, Y. L. Wu and Y. A. Yan, Int. J. Mod. Phys. A **15**, 1817 (2000).

[7] Y. A. Yan, Y. L. Wu and W. Y. Wang, Int. J. Mod. Phys. A **15**, 2735 (2000).

[8] W. Y. Wang and Y. L. Wu, Int. J. Mod. Phys. A **16**, 377 (2001).

[9] W. Y. Wang, Y. L. Wu, Phys. Lett. B **515** 57 (2001). (hep-ph/0105154)

[10] W. Y. Wang, Y. L. Wu, Phys. Lett. B **519** 219 (2001). (hep-ph/0106208)

[11] W. Y. Wang, Y. L. Wu and M. Zhong, hep-ph/0205157.

[12] N. Isgur and M. B. Wise, Phys. Rev. D **42**, 2388 (1990)

[13] G. Burdman and J. F. Donoghue, Phys. Lett. B **270**, 55 (1991).

[14] B. Stech, Phys. Lett. B **354** 447 (1995).

[15] J. M. Soares, Phys. Rev. D **54**, 6837 (1996).

[16] A. Ali, V. M. Braun, H. Simma, Z. Phys. C **63**, 437 (1994).

[17] J. Charles, A. Le Yaouanc, L. Oliver, O. Pène and J. C. Raynal, Phys. Rev. D **60**, 014001 (1999). (hep-ph/9812358)

[18] D. Ebert, R. N. Faustov and V. O. Galkin, Phys. Rev. D **64**, 094022 (2001).

[19] M. Beneke and Th. Feldmann, Nucl. Plys. B **592**, 3 (2001) (hep-ph/0008255)

[20] G. Kramer, G. A. Mannel, T. Schuler, Z. Phys. C **51**, 649 (1991)

[21] G. Burdman, Z. Ligeti, M. Neubert and Y. Nir, Phys. Rev. D **49**, 2331 (1994).

[22] C. S. Huang, C. Liu and C. T. Yan, Phys. Rev. D **62**, 054019 (2000).

[23] V. L. Chernyak and I. R. Zhitnitsky, Nucl. Phys. B **345**, 137 (1990)

[24] A. Khodjamirian and R. Rückl, Adv. Ser. Direct. High Energy Phys. **15**, 345 (1998) (WUE-ITP-97-049, MPI-PhT/97-85, hep-ph/9801443).

[25] V. M. Belyaev, A. Khodjamirian and R. Rückl, Z. Phys. C **60**, 349 (1993).

[26] P. Ball and V. M. Braun, Phys. Rev. D **55**, 5561 (1997).

[27] P. Ball and V. M. Braun, Phys. Rev. D **58**, 094016 (1998). (hep-ph/9805422)

[28] P. Ball, JHEP 09 (1998) 005

[29] P. Colangelo, F. De Fazio, P. Santorelli, and E. Scrimieri, Phys. Rev. D **53**, 3672 (1996).

[30] A. Khodjamirian, R. Rückl, S. Weinzierl, C. W. Winhart and O. Yakovlev, Phys. Rev. D **62**, 114002 (2000). (hep-ph/0001297).

[31] V. M. Belyaev, V. M. Braun, A. Khodjamirian and R. Rückl, Phys.Rev. D **51** 6177 (1995).

[32] V. M. Braun and I. B. Filyanov, Z. Phys, C **44**, 157 (1989).

[33] V. L. Chernyak and A. R. Zhitnitsky, Phys. Rep. **112**, 173 (1984).

[34] V. M. Braun and I. B. Filyanov, Z. Phys. C **48**, 239 (1990).

[35] P. Ball, JHEP 01 (1999) 010

[36] G. Burdman, G. Hiller, Phys. Rev. D **63**, 113008 (2001) (hep-ph/0112063).

[37] D. Melikhov, B. Stech, Phys. Rev. D **62**, 014006.

[38] UKQCD Collaboration, L. Del Debbio et al, Phys. Lett. B **416**, 392 (1998).

[39] A. Abada, D. Becirevic, Ph. Boucaud, J. P. Leroy, V. Lubicz, G. Martinelli, F. Mescia, Nucl. Phys. Proc. Suppl. **83**, 268 (2000) (hep-lat/9910021).

[40] Chuan-Hung Chen, C. Q. Geng, Nucl. Phys. B **636**, 338 (hep-ph/0203003).

[41] A. J. Buras, M. Münz, Phys. Rev. D **52**, 186 (1995)

[42] A. J. Buras, M. Misiak, M. Münz and S. Pokorski, Nucl. Phys. B **424**, 374 (1994)

[43] Belle Collaboration, K. Abe et al., Phys. Rev. Lett. **88(2)**,021801(6) (2002)

[44] CLEO Collaboration, T. E. Coan et al. Phys. Rev. Lett. **84**, 5283 (2000)

[45] G. Taylor,[BELLE Collaboration], talk presented at the 36th Rencontres de Moriond Electroweak Interactions and Unified Theories, Les Arcs, France, March 2001.

[46] Particle Data Group, D. E. Groom et al, EPJ C **15** 1 (2000)

FIGURES

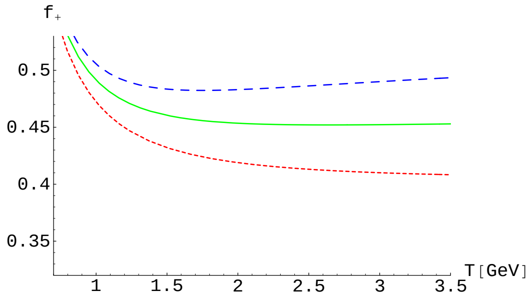

Fig.1 The form factors f_+ as functions of the Borel parameter T for different values of the threshold s_0. The dotted, solid and dashed curves correspond to $s_0 = 2.1, 2.4$ and 2.7GeV respectively. The momentum transfer is $q^2 = 0$.

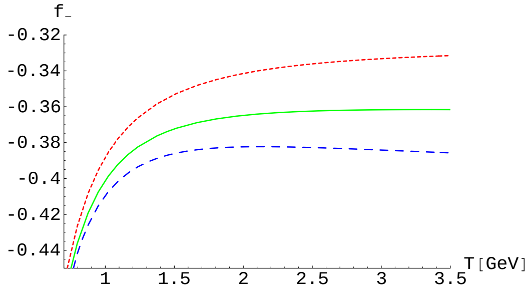

Fig.2 Same as Fig.1 but for f_-.

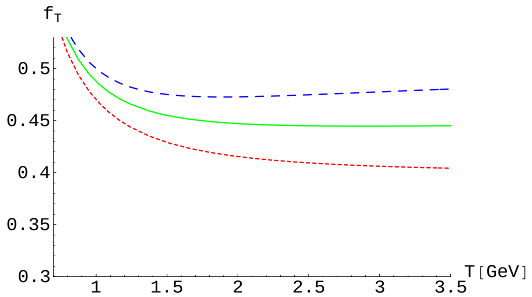

Fig.3 Same as Fig.1 but for f_T.

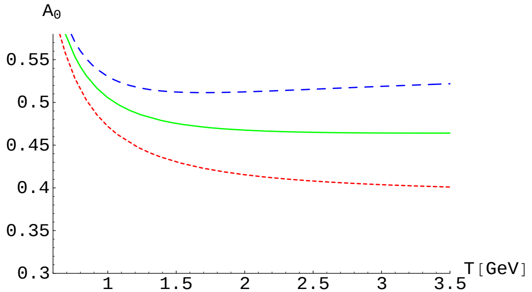

Fig.4 The form factors A_0 as functions of the Borel parameter T for different values of the threshold s_0. The dotted, solid and dashed curves correspond to $s_0 = 1.8, 2.1$ and 2.4GeV respectively. The momentum transfer is $q^2 = 0$.

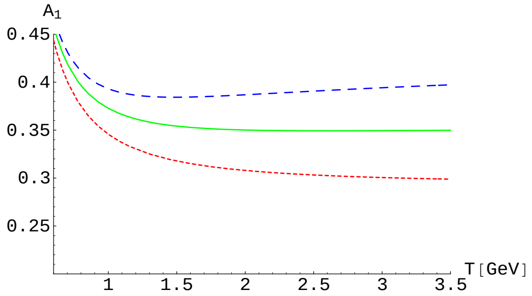

Fig.5 Same as Fig.4 but for A_1.

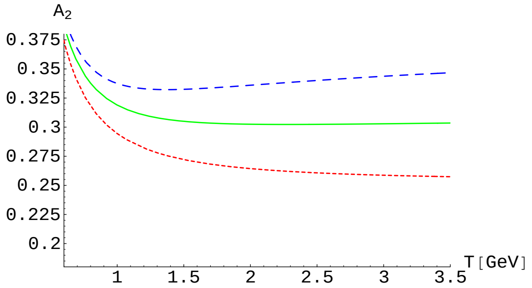

Fig.6 Same as Fig.4 but for A_2.

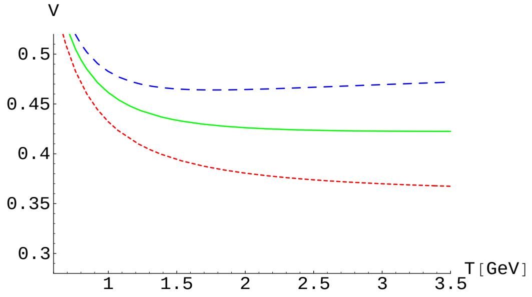

Fig.7 Same as Fig.4 but for V.

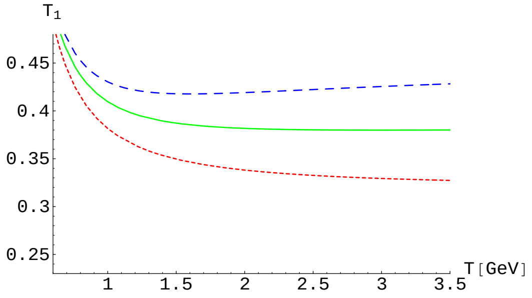

Fig.8 Same as Fig.4 but for T_1.

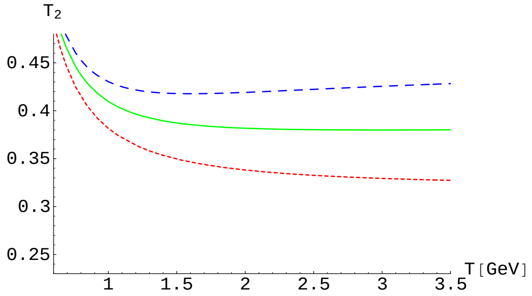

Fig.9 Same as Fig.4 but for T_2.

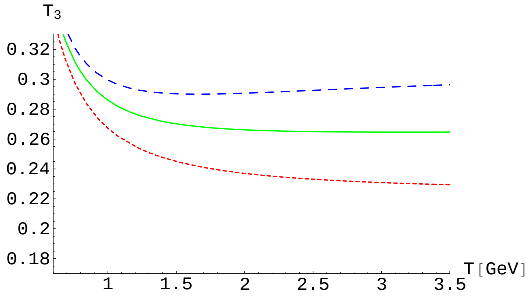

Fig.10 Same as Fig.4 but for T_3.

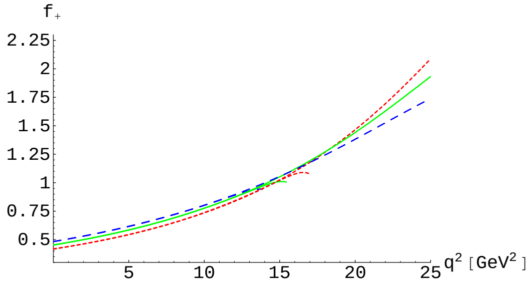

Fig.11 The form factors f_+ as functions of q^2 for different values of the threshold s_0. The dotted, solid and dashed curves correspond to $s_0 = 2.1, 2.4$ and 2.7GeV respectively.

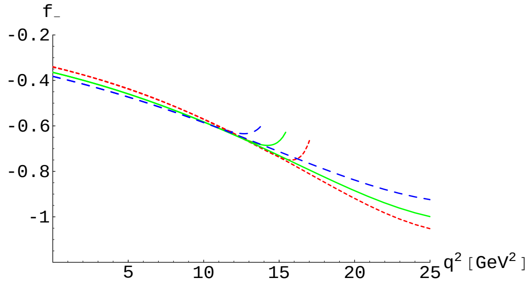

Fig.12 Same as Fig.11 but for f_-.

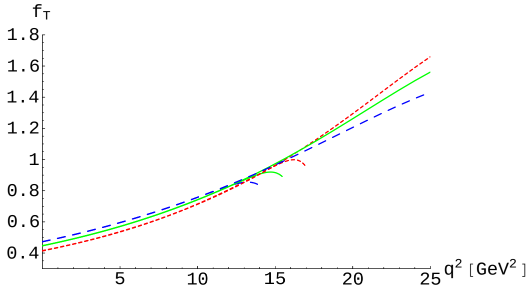

Fig.13 Same as Fig.11 but for f_T.

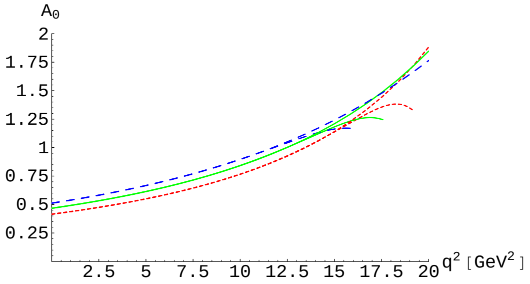

Fig.14 The form factors A_0 as functions of q^2 for different values of the threshold s_0. The dotted, solid and dashed curves correspond to $s_0 = 1.8, 2.1$ and 2.4GeV respectively.

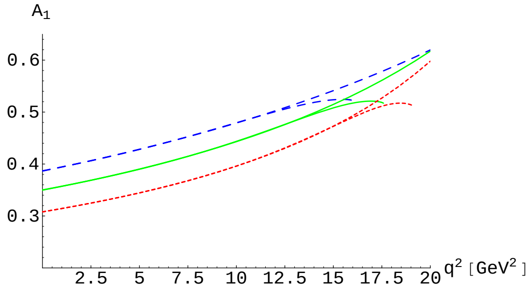

Fig.15 Same as Fig.14 but for A_1.

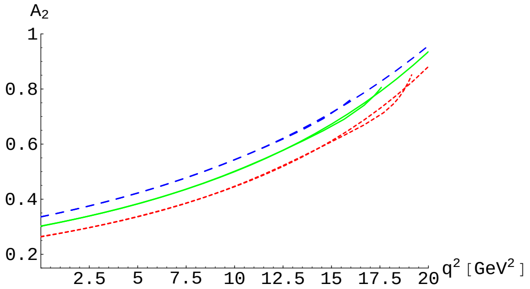

Fig.16 Same as Fig.14 but for A_2.

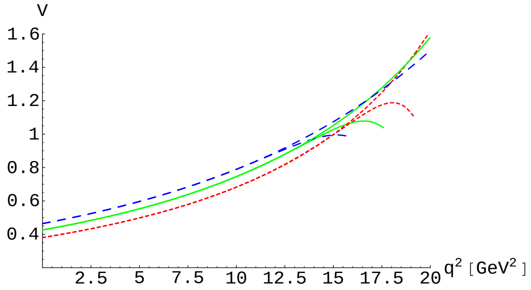

Fig.17 Same as Fig.14 but for V.

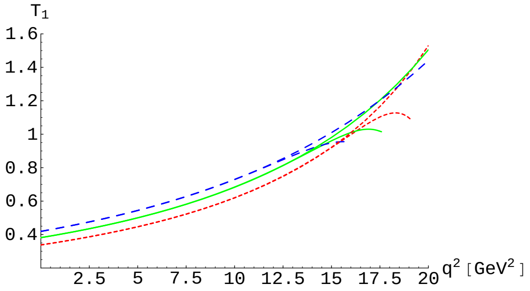

Fig.18 Same as Fig.14 but for T_1.

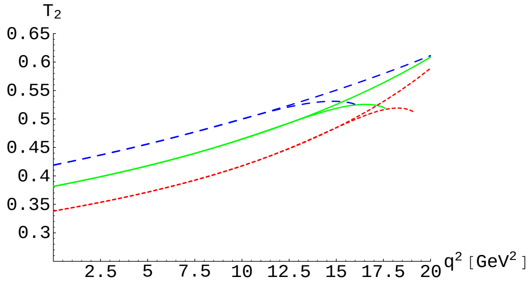

Fig.19 Same as Fig.14 but for T_2.

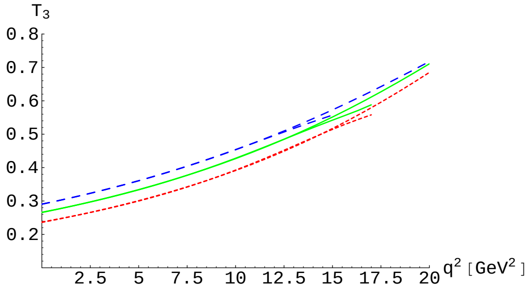

Fig.20 Same as Fig.14 but for T_3.

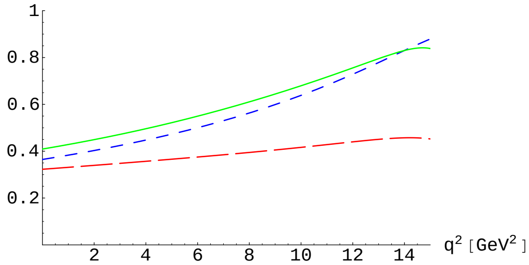

Fig.21 $\zeta_{\|}(q^2)$, $\zeta_{\perp}(q^2)$ and $\zeta(q^2)$ at center value of s_0 with $T = 2.0$GeV. The dotted, dashed and solid curves correspond to $\zeta_{\|}(q^2)$, $\zeta_{\perp}(q^2)$ and $\zeta(q^2)$ respectively.

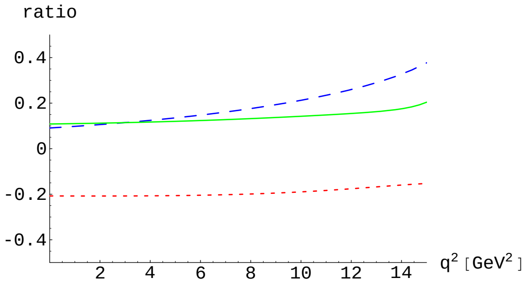

Fig.22 $\zeta_2(q^2)/\zeta_{\|}(q^2)$, $\zeta_1(q^2)/\zeta_{\perp}(q^2)$ and $\zeta_A(q^2)/\zeta(q^2)$ at center value of s_0 with $T = 2.0$GeV. The dotted, dashed and solid curves correspond to $\zeta_2(q^2)/\zeta_{\|}(q^2)$, $\zeta_1(q^2)/\zeta_{\perp}(q^2)$ and $\zeta_A(q^2)/\zeta(q^2)$ respectively.

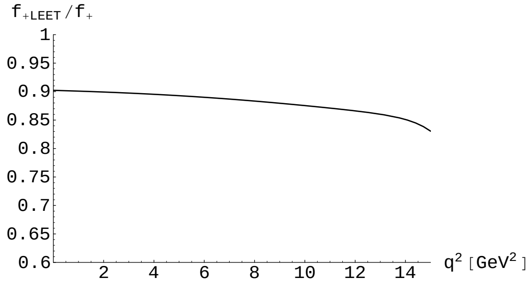

Fig.23 $f_{+LEET}(q^2)/f_+(q^2)$ at $s_0 = 2.4$GeV with $T = 2.0$GeV.

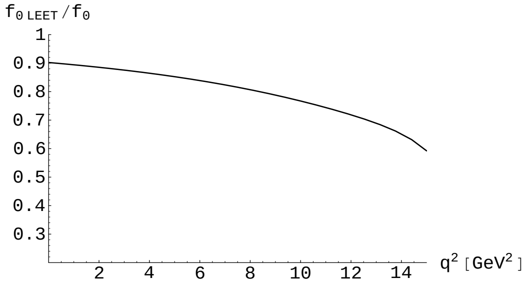

Fig.24 Same as Fig.23 but for $f_{-LEET}(q^2)/f_-(q^2)$.

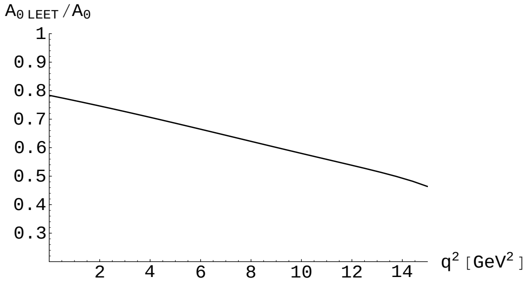

Fig.25 $A_{0LEET}(q^2)/A_0(q^2)$ at $s_0 = 2.1$GeV with $T = 2.0$GeV.

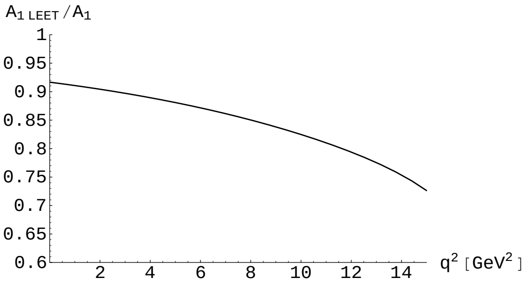

Fig.26 Same as Fig.25 but for $A_{1LEET}(q^2)/A_1(q^2)$.

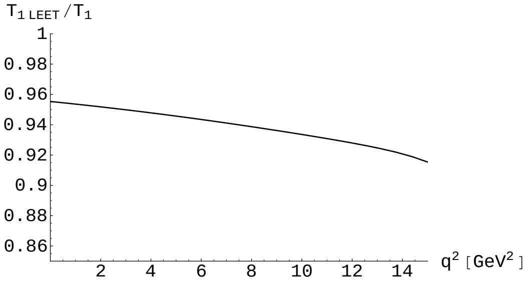

Fig.27 Same as Fig.25 but for $T_{1LEET}(q^2)/T_1(q^2)$.

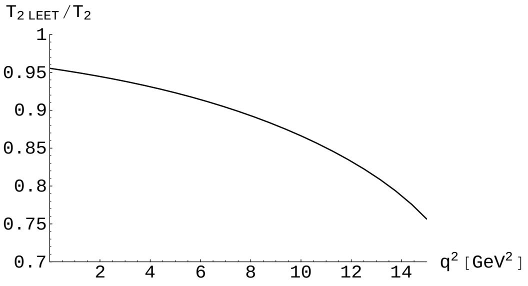

Fig.28 Same as Fig.25 but for $T_{2LEET}(q^2)/T_2(q^2)$.

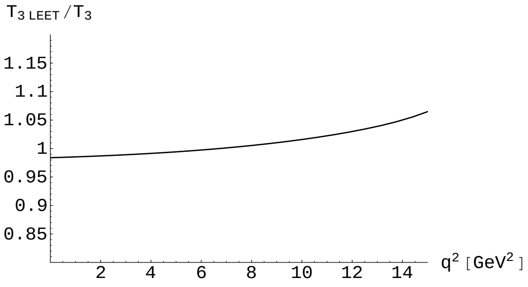

Fig.29 Same as Fig.25 but for $T_{3LEET}(q^2)/T_3(q^2)$.

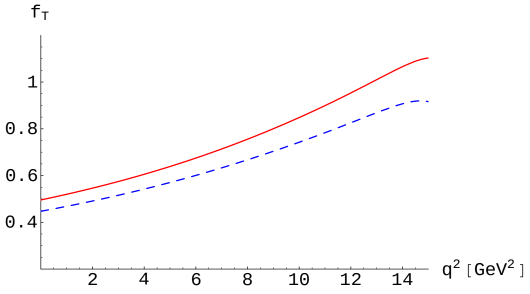

Fig.30 LEET relation (5.17) for $B \to K$ at $s_0 = 2.4$GeV and $T = 2.0$GeV. The dashed and solid curves correspond to LHS and RHS of the equation respectively.

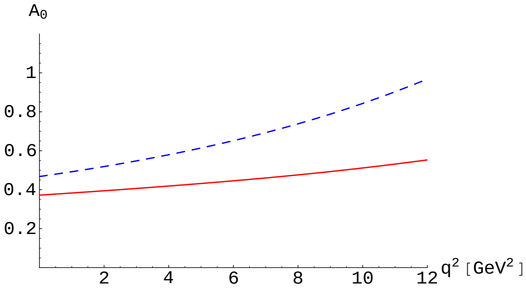

Fig.31 LEET relation (5.18) for $B \to K^*$ at $s_0 = 2.1$GeV and $T = 2.0$GeV. The dashed and solid curves correspond to LHS and RHS of the equation respectively.

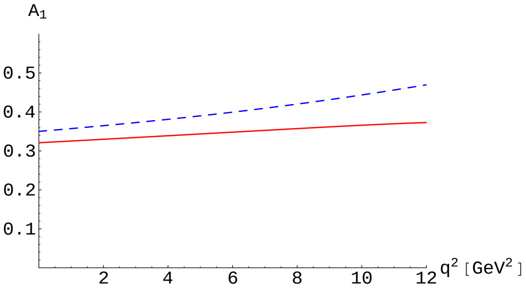

Fig.32 LEET relation (5.19) for $B \to K^*$ at $s_0 = 2.1$GeV and $T = 2.0$GeV. The dashed and solid curves correspond to LHS and RHS of the equation respectively.